Journal of Hydroscience and Hydraulic Engineering
Vol. 19, No.1 May, 2001, 53-64

STUDY ON PRESERVING THE NINOARATE WEIR BY FLOOD FLOW ANALYSIS OF THE HYAKKEN RIVER

By

Shiro MAENO

Department of Environmental and Civil Engineering, Okayama University
Tsushima-Naka, Okayama, 700-8530, Japan

SYNOPSIS

The Ninoarate weir of the Hyakken river is a historic civil engineering structure which was built more than three hundred years ago. Under the original river restoration plan, the entire Ninoarate weir structure was scheduled to be removed. However, due to the historic significance of this precious hydraulic structure, the possibility of its preservation has been re-examined in recent years. In this paper, the possibility of preserving the Ninoarate weir is studied by the flood flow analysis based on the MacCormack Scheme. Numerical results show that it is feasible to preserve a part of the Ninoarate weir at the actual location, though it may be difficult to preserve the whole structure.

INTRODUCTION

The Hyakken river is a diversion channel of the Asahi river to protect Okayama city from flood disaster. Banzan Kumazawa who was a political advisor of the Okayama clan originally devised the idea of this diversion channel. According to his idea, Eichu Tsuda who was the county reign of the Okayama clan constructed it. When the flood of the Asahi river is about to inundate Okayama city, the flood overflows the weir constructed upstream of the Asahi river to protect Okayama city. This weir is called the Ichinoarate weir (see Fig.1). In the Hyakken river, two other overflow type weirs were originally constructed in 1686 (see Histroy of the Hyakken river (1)). These weirs were built across the Hyakken river to reduce the flood energy and to accelerate the sedimentation. These weirs are called the Ninoarate weir (see Fig.1) and the Sannoarate weir respectively. The Hyakken river has protected Okayama city from flood disaster for more than three hundred years. Although the Sannoarate weir was destroyed by the heavy flood in 1892, the Ninoarate weir is well preserved in its original form. As shown in Photo 1 and 2, a highly skillful technique was used in its masonry work. The name of the Hyakken river was derived from the width of the Ninoarate weir, which was 100 ken (100 ken is called hyakken in Japanese and its length is about 180m). The length of the weir along the Hyakken river is about 20m. Therefore, the Ninoarate weir is considered to be worth preserving as a historic civil engineering structure. Under the original plan for river restoration, the designed flood discharge for the Hyakken river is 2000m^3/s and that for the main river (the Asahi river) is 4000m^3/s. According to this plan, construction work has been carried out and the entire Ninoarate weir structure is scheduled to be removed. However, due to the historic significance of this precious hydraulic structure, the

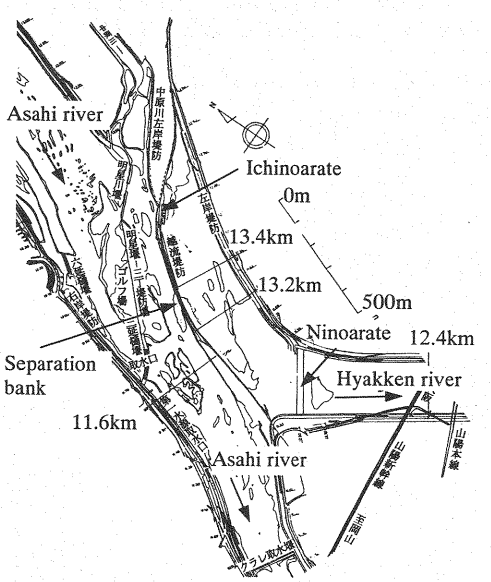

Fig. 1 The Asahi river and the Hyakken river

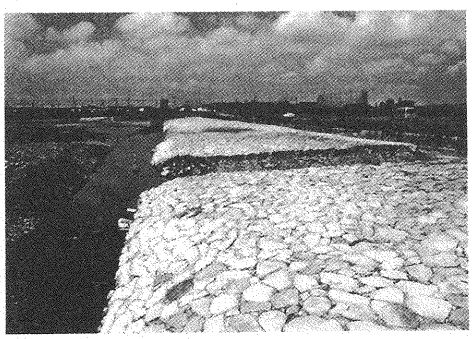

Photo 1 Overflow bank (central part of the Ninoarate weir)

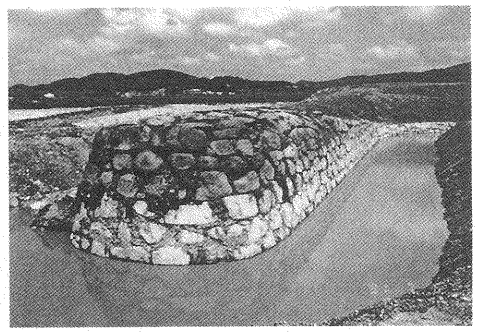

Photo 2 Training dike (left hand side of the Ninoarate weir)

possibility of its preservation has been re-examined recently. In this work, the possibility of preserving the Ninoarate weir is studied by the flood flow analysis. In the numerical analysis, two dimensional St. Venant shallow water equations (see Chow (2) and Garcia et al. (3)) were used and a generalized curvilinear co-ordinate system (see Shimizu et al. (4)) was adopted considering the curvature of the Hyakken river. Since supercritical flow and subcritical flow are expected to appear around the Ninoarate weir, MacCormack time splitting scheme (see Garcia et al. (3), Shimizu et al. (4) and Daiguji et al. (5)) which is generally applicable to such kind of severe flow conditions was adopted as a numerical method.

OUTLINE OF NUMERICAL ANALYSIS

Basic equations

Two-dimensional St. Venant shallow water equations in a generalized curvilinear coordinate system were used (see Shimizu et al. (4)).

$$\mathbf{A}_t + \mathbf{B}_\xi + \mathbf{C}_\eta = \mathbf{D}^\xi + \mathbf{D}^\eta + \mathbf{R}_\xi + \mathbf{T}_\eta \tag{1}$$

$$\mathbf{A} = \begin{bmatrix} \dfrac{h}{J} \\ \dfrac{uh}{J} \\ \dfrac{vh}{J} \end{bmatrix} \quad \mathbf{B} = \begin{bmatrix} \dfrac{u'h}{J} \\ \dfrac{1}{J}\left[\left(u'uh\right) + \dfrac{\xi_x}{2} gh^2\right] \\ \dfrac{1}{J}\left[\left(u'vh\right) + \dfrac{\xi_y}{2} gh^2\right] \end{bmatrix} \quad \mathbf{C} = \begin{bmatrix} \dfrac{v'h}{J} \\ \dfrac{1}{J}\left[\left(v'uh\right) + \dfrac{\eta_x}{2} gh^2\right] \\ \dfrac{1}{J}\left[\left(v'vh\right) + \dfrac{\eta_y}{2} gh^2\right] \end{bmatrix}$$

$$\mathbf{D}^\xi = \begin{bmatrix} 0 \\ \dfrac{1}{J} gh(-\xi_x \dfrac{\partial z}{\partial \xi} - \dfrac{\eta_y}{J} u' \dfrac{n^2\sqrt{u^2+v^2}}{h^{4/3}}) \\ \dfrac{1}{J} gh(-\xi_y \dfrac{\partial z}{\partial \xi} - \dfrac{\eta_x}{J} u' \dfrac{n^2\sqrt{u^2+v^2}}{h^{4/3}}) \end{bmatrix} \quad \mathbf{D}^\eta = \begin{bmatrix} 0 \\ \dfrac{1}{J} gh(-\eta_x \dfrac{\partial z}{\partial \eta} - \dfrac{\xi_y}{J} v' \dfrac{n^2\sqrt{u^2+v^2}}{h^{4/3}}) \\ \dfrac{1}{J} gh(-\eta_y \dfrac{\partial z}{\partial \eta} - \dfrac{\xi_x}{J} v' \dfrac{n^2\sqrt{u^2+v^2}}{h^{4/3}}) \end{bmatrix}$$

$$\mathbf{R} = \begin{bmatrix} 0 \\ \varepsilon\left\{(\xi_x^2+\xi_y^2)\dfrac{\partial(uh)}{\partial\xi} + (\xi_x\eta_x+\xi_y\eta_y)\dfrac{\partial(uh)}{\partial\eta}\right\} \\ \varepsilon\left\{(\xi_x^2+\xi_y^2)\dfrac{\partial(vh)}{\partial\xi} + (\xi_x\eta_x+\xi_y\eta_y)\dfrac{\partial(vh)}{\partial\eta}\right\} \end{bmatrix} \quad \mathbf{T} = \begin{bmatrix} 0 \\ \varepsilon\left\{(\eta_x^2+\eta_y^2)\dfrac{\partial(uh)}{\partial\eta} + (\xi_x\eta_x+\xi_y\eta_y)\dfrac{\partial(uh)}{\partial\xi}\right\} \\ \varepsilon\left\{(\eta_x^2+\eta_y^2)\dfrac{\partial(vh)}{\partial\eta} + (\xi_x\eta_x+\xi_y\eta_y)\dfrac{\partial(vh)}{\partial\xi}\right\} \end{bmatrix}$$

Here, x, y : axes in Cartesian coordinates, ξ, η : axes in curvilinear coordinates, J : Jacobean of coordinate transform $(J = \xi_x\eta_y - \xi_y\eta_x)$, h : water depth, z : bed level, u, v : velocities in x, y direction, u', v' : velocities in ξ, η direction (contravariant velocities), g : gravity acceleration, ε : coefficient of eddy viscosity, n : coefficient of Manning's roughness.

Table 1 Finite difference manner in each step

Step	Predictor stage	Corrector stage
First step L_ξ	Backward difference	Forward difference
Second step L_η	Backward difference	Forward difference
Third step L_η	Forward difference	Backward difference
Fourth step L_ξ	Forward difference	Backward difference

MacCormack numerical scheme

The MacCormack time splitting scheme, which is one of the explicit finite difference methods, was used in the numerical analysis. This scheme is a fractional step method where a complicated two-dimensional finite difference operator is split into a sequence of simpler one-dimensional operators. That is, the basic Eqs.(1) are split into a sequence of ξ and η directions of finite difference operator as shown in Eqs.(2.1) and Eqs.(2.2). Each operator is composed of a predictor and corrector stages. The discretized derivatives in Eqs.(2.1) and Eqs.(2.2) are the first order accuracy. To retain the second order accuracy in space and time, Garcia and Kahawita proposed a cyclic symmetrical discretization of derivatives as shown in Table 1. In this method, to improve the accuracy of the calculation, the forward and backward difference calculations are reversed to each other in predictor and corrector stages.

ξ direction operator : L_ξ

Predictor stage (backward difference : $m=0$, forward difference : $m=1$)

$$\mathbf{A}^p_{i,j}=\mathbf{A}^n_{i,j}-\frac{\Delta t}{\Delta\xi}(\mathbf{B}^n_{i+m,j}-\mathbf{B}^n_{i+m-1,j})+\Delta t\cdot\mathbf{D}^n_{\xi i,j}+\Delta t\cdot\mathbf{R}^n_{\xi i,j}$$

Corrector stage (backward difference : $m=0$, forward difference : $m=1$)

$$\mathbf{A}^c_{i,j}=\mathbf{A}^p_{i,j}-\frac{\Delta t}{\Delta\xi}(\mathbf{B}^p_{i+m,j}-\mathbf{B}^p_{i+m-1,j})+\Delta t\cdot\mathbf{D}^p_{\xi i,j}+\Delta t\cdot\mathbf{R}^p_{\xi i,j}$$

$$\mathbf{A}^{n+1}_{i,j}=\frac{1}{2}(\mathbf{A}^n_{i,j}+\mathbf{A}^c_{i,j}) \tag{2.1}$$

η direciton operator : L_η

Predictor stage (backward difference : $m=0$, forward difference : $m=1$)

$$\mathbf{A}^p_{i,j}=\mathbf{A}^n_{i,j}-\frac{\Delta t}{\Delta\eta}(\mathbf{C}^n_{i,j+m}-\mathbf{C}^n_{i,j+m-1})+\Delta t\cdot\mathbf{D}^n_{\eta i,j}+\Delta t\cdot\mathbf{T}^n_{\eta i,j}$$

Corrector stage (backward difference : $m=0$, forward difference : $m=1$)

$$\mathbf{A}^c_{i,j}=\mathbf{A}^p_{i,j}-\frac{\Delta t}{\Delta\eta}(\mathbf{C}^p_{i,j+m}-\mathbf{C}^p_{i,j+m-1})+\Delta t\cdot\mathbf{D}^p_{\eta i,j}+\Delta t\cdot\mathbf{T}^p_{\eta i,j}$$

$$\mathbf{A}^{n+1}_{i,j}=\frac{1}{2}(\mathbf{A}^n_{i,j}+\mathbf{A}^c_{i,j}) \tag{2.2}$$

In every small time step, the above mentioned cyclic symmetrical 4 step calculation must be repeated. Courant-Friederichs-Lewy's stability conditions were used in the calculation.

$$\Delta t=\min\left(\frac{C_r\Delta\xi}{\max(|u'|+|\xi_x+\xi_y|\sqrt{gh})},\ \frac{C_r\Delta\eta}{\max(|v'|+|\eta_x+\eta_y|\sqrt{gh})}\right) \tag{3}$$

Here, C_r is a Courant number.

MacCormack scheme produces numerical oscillation near discontinuities when it is applied to the coexisted flow with subcritical flow and supercritical flow. It is necessary to add an artificial viscosity term to prevent a numerical dissipation. In this study, the procedure developed by Jameson et al. (6) was adopted. In this paper, following eddy coefficient was used to match a generalized

Table 2 Numerical conditions

Initial water level	$h = 8.4\ (m)$
Initial velocity	$v_x = v_y = 0\ (m/s)$
Discharge (upstream boundary)	$Q = 2000 \times n/1000\ \ (\mathrm{m}^3/s) : n < 1000\mathrm{step}$ $Q = 2000\ \ (\mathrm{m}^3/s) : n \geq 1000\mathrm{step}$
Water level (downstream boundary)	$h = 8.4\ (m)$ (mean value of the experimentally obtained data)
Courant number	$C_r = 0.9$
Coefficient of Manning's roughness	$n = 0.03$
Coefficient of eddy viscosity	$\varepsilon = \alpha u_* h \quad (\alpha = \kappa/6.0,\ \ \kappa = 0.4)$
Damping parameter used in artificial viscosity term	$k = 0.20$

curvilinear coordinate system, whereas the expression of the artificial viscosity term in Fennema and Chaudhry (7), Akiyama et al. (8) was for the Cartesian coordinate.

ξ direction :

$$\mathbf{A}_{i,j}^{n+1} = \mathbf{A}_{i,j}^{n+1} + [\gamma_{\xi\, i+1/2,j}(\mathbf{A}_{i+1,j}^{n+1} - \mathbf{A}_{i,j}^{n+1}) - \gamma_{\xi\, i-1/2,j}(\mathbf{A}_{i,j}^{n+1} - \mathbf{A}_{i-1,j}^{n+1})]$$

η direction :

$$\mathbf{A}_{i,j}^{n+1} = \mathbf{A}_{i,j}^{n+1} + [\gamma_{\eta\, i,j+1/2}(\mathbf{A}_{i,j+1}^{n+1} - \mathbf{A}_{i,j}^{n+1}) - \gamma_{\eta\, i,j-1/2}(\mathbf{A}_{i,j}^{n+1} - \mathbf{A}_{i,j-1}^{n+1})]$$

Here,

$$\gamma_{\xi_{i-1/2,j}} = k\max(\nu_{\xi_{i-1}},\ \nu_{\xi_i}),\quad \gamma_{\eta\, i,j-1/2} = k\max(\nu_{\eta\, i-1},\ \nu_{\eta\, i})$$

(k :coefficient of artificial viscosity)

$$\nu_{\xi\, i,j} = \frac{\left|\frac{h_{i+1,j}-h_{i,j}}{\ell_{\xi\, i+1/2,j}} - \frac{h_{i,j}-h_{i-1,j}}{\ell_{\xi\, i-1/2,j}}\right| \cdot \ell_{\xi_{i,j}}}{h_{i+1,j} + 2h_{i,j} + h_{i-1,j}},\qquad \nu_{\eta\, i,j} = \frac{\left|\frac{h_{i,j+1}-h_{i,j}}{\ell_{\eta\, i,j+1/2}} - \frac{h_{i,j}-h_{i,j-1}}{\ell_{\eta\, i,j-1/2}}\right| \cdot \ell_{\eta_{i,j}}}{h_{i+1,j} + 2h_{i,j} + h_{i-1,j}}$$

$$\ell_{\xi\, i,j} = \sqrt{x_{\xi_{i,j}}^2 + y_{\xi_{i,j}}^2},\quad \ell_{\eta\, i,j} = \sqrt{x_{\eta_{i,j}}^2 + y_{\eta_{i,j}}^2}$$

Numerical conditions

Numerical conditions are shown in Table 2. Initial water level and velocities are given to the whole analytical domain. The upstream discharge increases until a predetermined time step. After that the calculations were continued until the discharge of downstream boundary became steady.

Fig.2 shows a plan view of the analytical domain, which is located between 12.4km to 13.4km from the mouth of the Hyakken river. The Ninoarate weir is shown as a dotted line. It is located 12.8km+45m from the river mouth.

Fig.3 shows the mesh grid used in the calculation. The analytical domain was divided into 6729 (40×168) meshes. Four cases of numerical analysis were carried out as shown in Table 3. Fig. 4 shows the preserved part of the Ninoarate weir for Case 2, 3, 4. That is, Case1 is the originally designed section. In this case, the whole entire structure of the Ninoarate weir is assumed to be removed. Case4 is assumed to preserve the whole section of the Ninoarate weir. In Case2, only the training dike (Section I) is assumed to be preserved. In Case3, the right hand side of the Ninoarate weir (Section III) is preserved in addition to Case2. In Case2 and Case3, central part of the Ninoarate weir (Section II) is removed until the designed bed level of the lower channel. In Fig.4, the river-bed form for Case4 is shown.

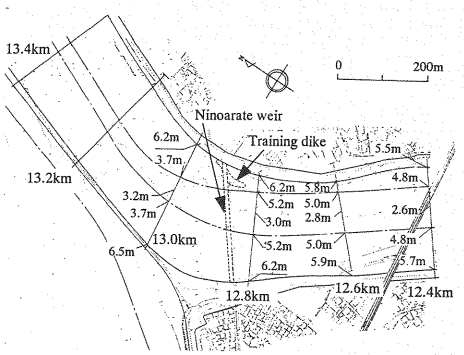

Fig. 2 Plan view of the analytical domain

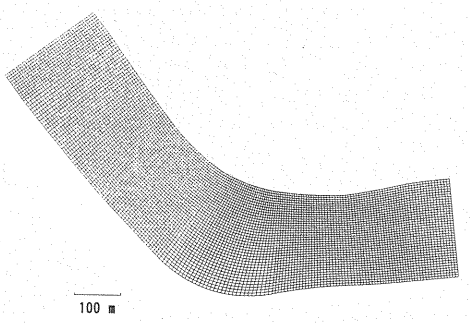

Fig. 3 Mesh grid used in the analysis

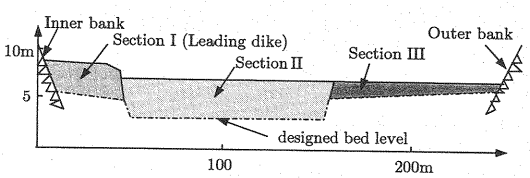

Fig. 4 Preserved part for Case2, 3, 4

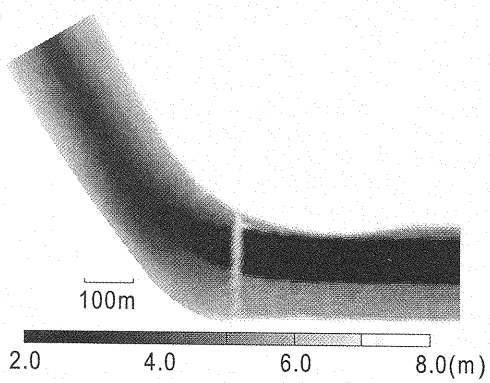

Fig. 5 Bed level profile for Case4

Table 3 Numerical conditions

Case	Bed level conditions
1	No Ninoarate weir (designed bed level)
2	Section I kept, Section II and III removed
3	Section I and III kept, Section II removed
4	Ninoarate weir as it is

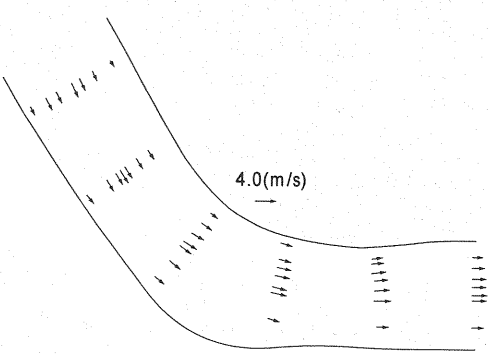

Fig. 6 Velocity distribution for Case1 (Experimnent)

RESULTS AND DISCUSSIONS

Model Application

Public Works Research Institute of the Ministry of Construction carried out the 1 to 50 scale model test for Case1 (see Report of Experiments on the Asahi river (9)). Therefore, applicability of the numerical model was examined by comparing numerical results and experimental results for Case1. Fig.6 shows the experimentally obtained velocity distribution for Case1.

Fig.7 shows the water level profiles for Case1 in which the entire Ninoarate weir is removed.

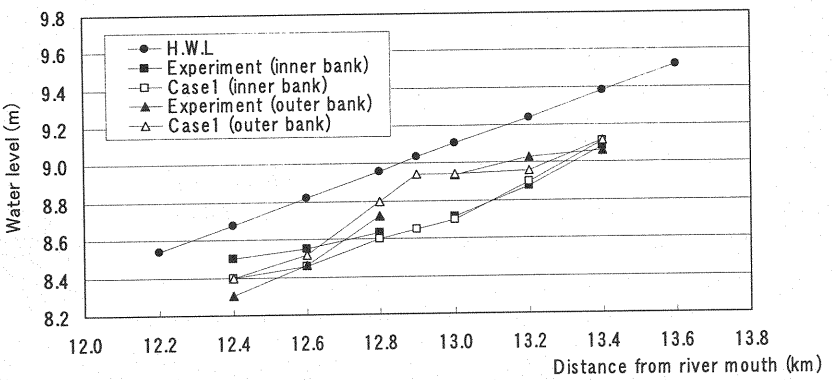

Fig. 7 Water level profile for Case1 (designed bed level)

The water level of the outer bank is higher than that of the inner bank at the river bending section (around 12.9 km from the river mouth). This feature known as superelevation shows a good agreement with the experimental result. Although the water level of the outer bank at section 13.2 km becomes higher than the experimental result, the water levels of both sides of the banks at section 13.0 km show in good agreement with experimental data. In the vicinity of the downstream boundary, the water level of the outer bank becomes higher than that of the experimental result. This result is mainly caused by the downstream boundary conditions, that is, the water level given at this boundary is fixed to a mean value of the experimentally obtained data. The water level never becomes higher than the designed high water level for this Case1. That means the flood flow can easily pass without formation of any critical state.

Fig.8 shows the water level distribution and the velocity distribution of the calculated domain. The water surface and the bed surface profiles are shown as a bird view.

As described above superelevation phenomenon appears at the outer bank, but the flood flow is very smooth. The velocity distribution shows that the flood flow of the bending area is also very smooth. The velocities of the main channel are higher than that of the side channels. The numerical results show in good agreement with the experimental results.

Considering the numerical results for Case1, it is clear that the numerical method used in the calculation is appropriate.

Study on a preservation of the Ninoarate weir

(a) Velocity and water level

Fig.9～Fig.11 show the results for Case2～Case4, respectively. From these figures, the followings are clarified.

In Case 4, which is assumed to preserve whole section of the Ninoarate weir, the velocities and the water level are severely disturbed by the preserved part. A very high velocity field appears over the Ninoarate weir. The effect of the high velocity flow at side channels reaches as far as the downstream boundary. The backwater effect from the Ninoarate weir extends far upstream to the boundary and a remarkable drop in water surface occurs over the Ninoarate weir. In Case2 and Case3, which are assumed to preserve a part of the Ninoarate weir, the drop in water surface over the preserved Ninoarate weir is not so severe as compared to Case4. And also the disturbed flow disappears rapidly and does not reach to the downstream boundary. The magnitude of the velocities around the preserved part becomes much smaller than Case4. The general behavior of the flood flow for Case2 and 3 are almost similar to Case1 except for the flow profiles around the preserved part.

(b) Flow profile and Hydraulic quantities over the Ninoarate weir

Fig.12 and 13 show the water level profile of inner side bank and outer side bank, respectively. Fig.14 shows the flow profiles over the training dike, over the central part and right side of the Ninoarate weir. Table 4 shows hydraulic quantities of these parts.

In Case4 the elevation of backwater caused by the Ninoarate weir exceeds the designed high water level. The velocity at the central part of the Ninoarate weir reaches up to 7.6(m/s). Froude number exceeds 2 and severe supercritical flow occurs. Furthermore, hydraulic jump occurs over the Ninoarate weir and an undular jump can be seen over the training dike. In Case2 and Case3, which

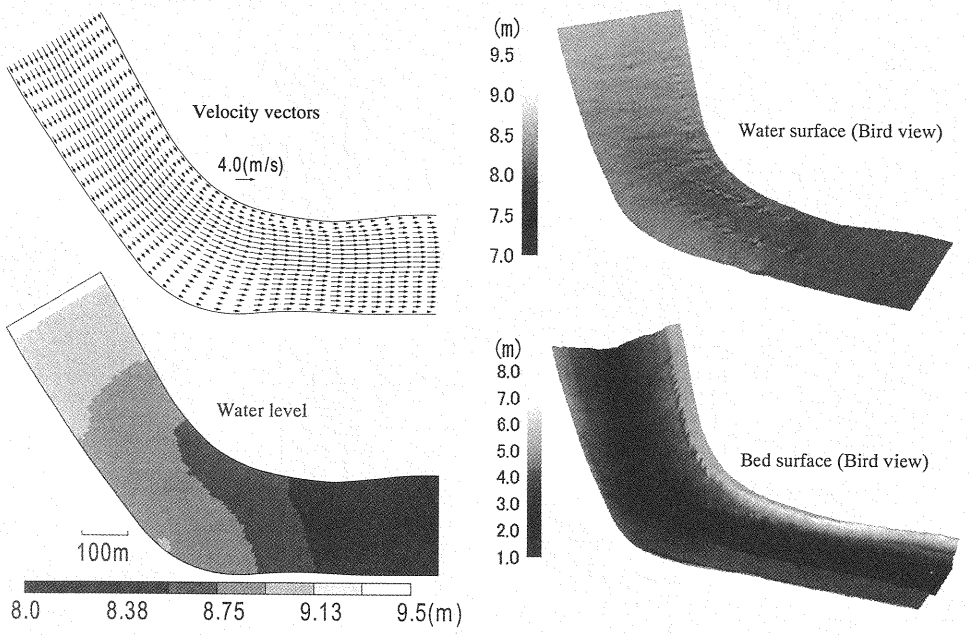

Fig. 8 Water level and velocity distribution (Case1)

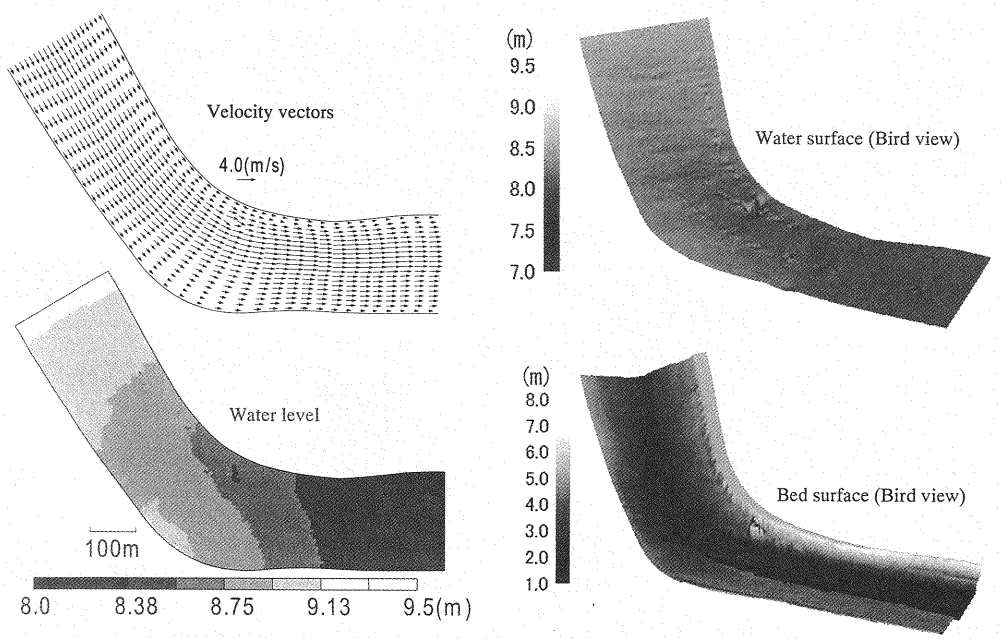

Fig. 9 Water level and velocity distribution (Case2)

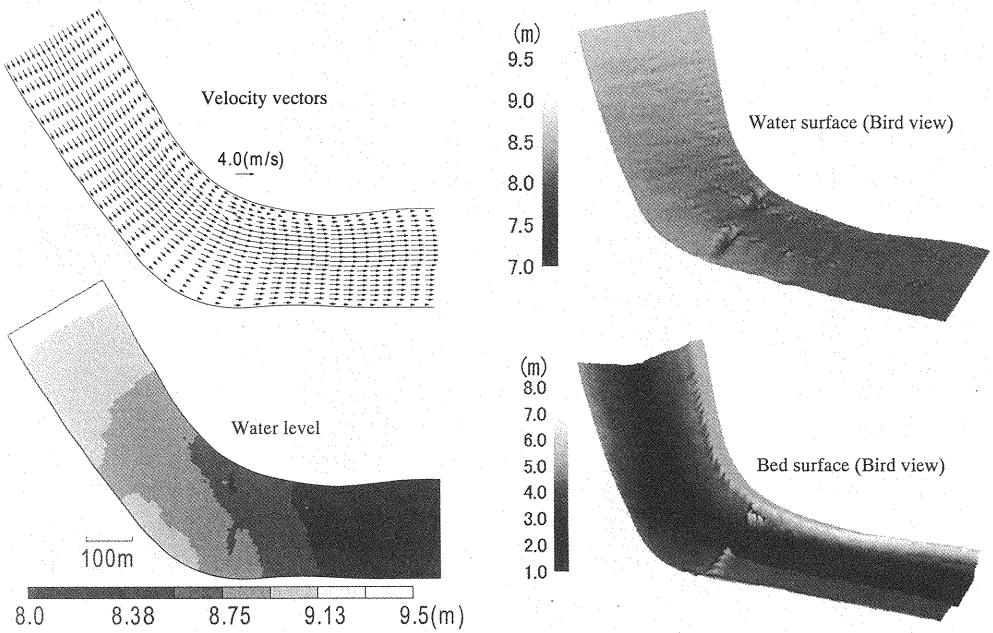

Fig. 10 Water level and velocity distribution (Case3)

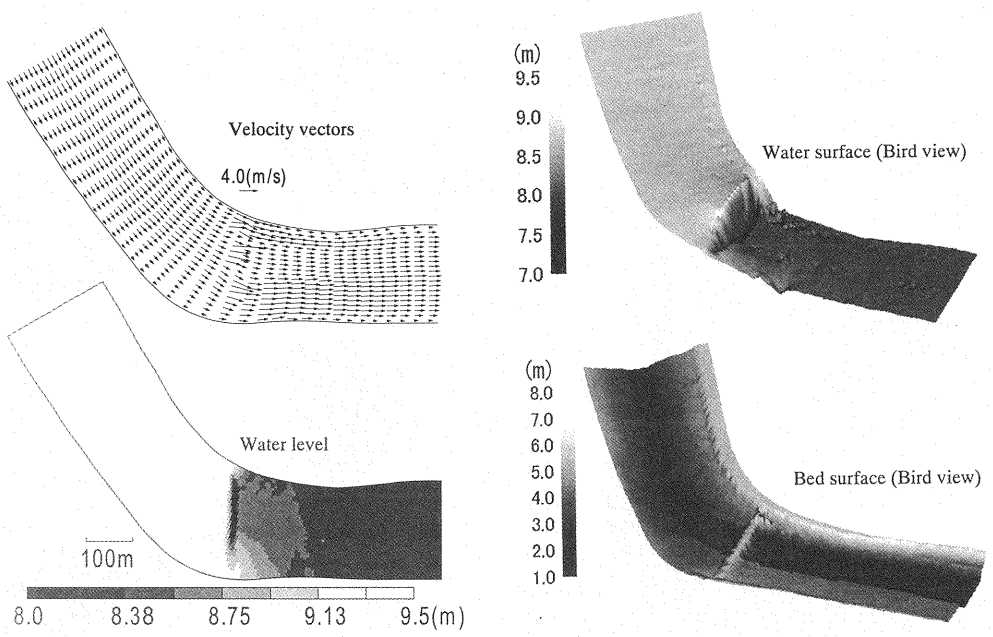

Fig. 11 Water level and velocity distribution (Case4)

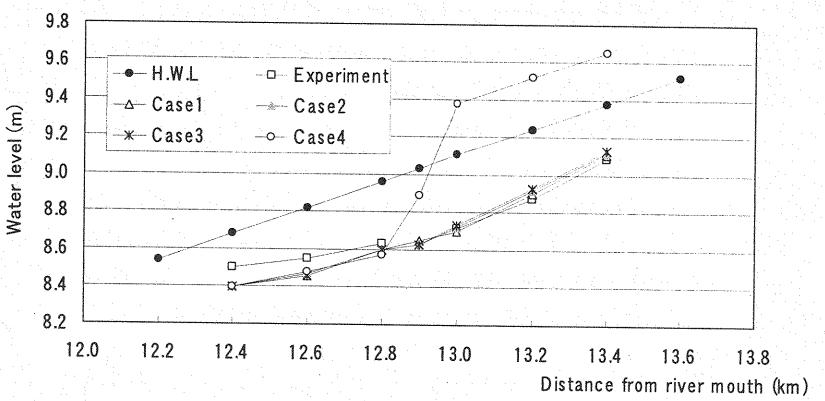

Fig. 12 Water level profile (inner side bank)

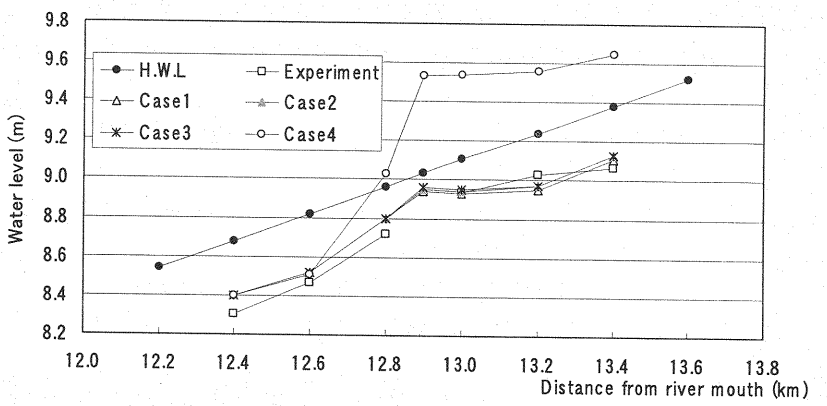

Fig. 13 Water level profile (outer side bank)

Table 4 Hydraulic quantities around the Ninoarate weir

Case	Hydraulic quantities	Water level(m)		Velocity(m/s)		Froude number	
	Position	Minimum	Max	Minimum	Max	Minimum	Max
1	Side channel (inner side)	8.64	8.69	2.03	2.17	0.34	0.38
	Main channel (Central part)	8.75	8.78	2.48	2.61	0.33	0.35
	Side channel (outer side)	8.80	8.89	1.66	1.91	0.29	0.35
2	Training dike	8.54	8.74	1.28	2.63	0.22	0.64
	Central part of the Ninoarate	8.72	8.77	2.67	2.75	0.36	0.37
	Right hand side of the Ninoarate	8.81	8.89	1.56	1.85	0.28	0.34
3	Training dike	8.54	8.74	1.28	2.65	0.22	0.68
	Central part of the Ninoarate	8.71	8.77	2.70	2.80	0.36	0.33
	Right hand side of the Ninoarate	8.72	8.90	1.53	2.33	0.27	0.50
4	Training dike	8.22	9.40	1.71	5.54	0.27	1.60
	Central part of the Ninoarate	7.64	9.53	1.29	7.61	0.17	2.27
	Right hand side of the Ninoarate	8.83	9.39	2.10	3.83	0.35	0.80

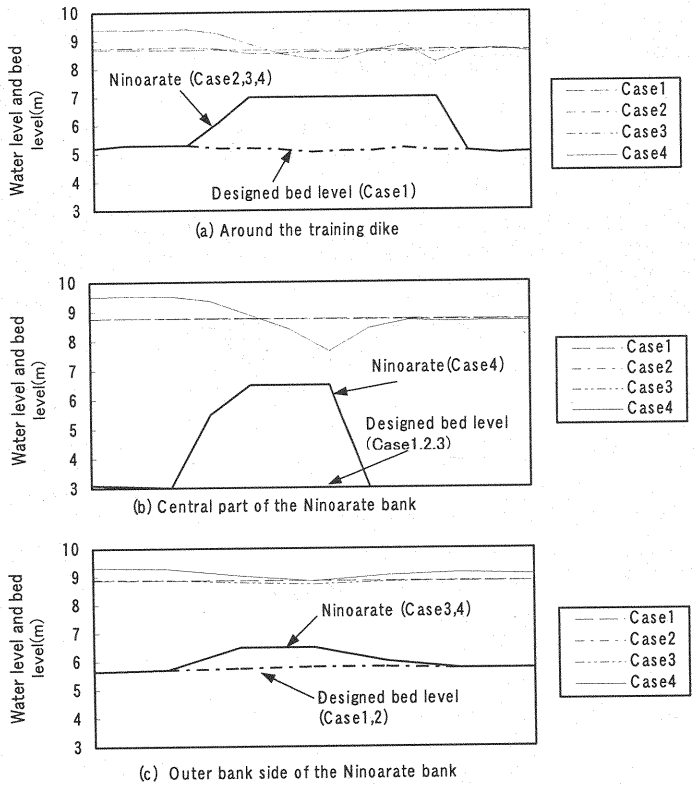

Fig. 14 Flow profiles over the Ninoarate weir

are the cases to preserve the part of the Ninoarate weir, the water level just upstream of the Ninoarate weir (13.0km-13.2km) is slightly higher than that of Case1. The difference in water level is just a few centimeters. Effect of removing the central part of the Ninoarate weir (Section II in Fig. 4) is remarkable. In Case3, the water level of the outer bank becomes almost the same as the designed high water level. But it does not exceed the designed high water level. In Case2 and Case3, the Froude numbers and the velocities over the preserved parts become larger than those of Case1. Such a severe supercritical flow like Case4 does not occur in these cases. Flow profiles over the training dike are disturbed to some extent, but not so severe compared to Case4.

Since the flow around the Ninnoarate weir is considerably disturbed in Case4, it is considered to be very difficult to preserve the whole section of it at the actual location. In Case2 and Case3, it is feasible to preserve a part of the Ninoarate weir considering the flood flow capacity. Even in these cases, the local scour caused by the disturbed flow may cause not only the destruction of the Ninoarate weir but also the failure of the main bank of the Hyakken river. So, it is necessary to take some scour protection measures when examining the preservation method.

CONCLUSIONS

In this study, the possibility of preserving the Ninoarate weir, which is a historic civil engineering structure built more than three hundred years ago, is studied by the flood flow analysis based on MacCormack Scheme. As a result, the following conclusions are obtained.

(1) It is clarified that the MacCormack numerical modeling in a generalized curvilinear coordinate system adopted in this study is appropriate to estimate the flood flow of the meandering river with subcritical and supercritical flow.

(3) It is considered to be very difficult to preserve the whole section of the Ninoarate weir taking into account the velocity distribution and the water level profile of the flood flow.

(3) If only the flood capacity is under consideration, it is feasible to preserve the training dike and right

hand side of the Ninoarate weir.

In this study, the analytical domain of the flood flow analysis is limited to a certain region of the Hyakken river. In the future study, it is necessary to extend the analytical domain including the Asahi river and the Ichinoarate weir.

ACKNOWLEDGMENT

This study was partly supported by a Grant of Electric Technology Research Foundation of Chugoku. The author would like to express gratitude.

REFERENCES

1. History of the Hyakken river : Okayama River Works Office, Ministry of Construction, 1992. (in Japanese)
2. Chow, V.T. Open-channel hydraulics : McGraw-Hill Book Co., Inc., New York, N.Y., 1959.
3. Garcia R. and R.A. Kahawita : Numerical solution of the St. Venant equations with the MacCormack finite difference scheme, International Jour. For Numerical Methods in Fluids, Vol.6, pp.259-274, 1986.
4. Shimizu Y., Y. Yamashita, S. Yamashita and N. Muneta : Computation of co-existing super-critical and sub-critical flows in a generalized curvilinear co-ordinate system, Report of Civil Engineering Research Institute, Hokkaido Development Bureau, No.455, pp.18-33, 1991. (in Japanese)
5. Daiguji H., N. Hirose, E. Ohta, M. Ikegawa, K. Kamemoto, T. Nishiyama, Y. Miyake and H. Ishigaki : Fundamentals of Computational Fluid Dynamics, JSME, Corona Publishing co., LTD, 1998. (in Japanese)
6. Jameson, A., Schmidt, W. and Turkel, E. : Numerical solutions of the Euler equations by finite volume methods using Runge-Kutta time-stepping schemes, Proc. AIAA 14th Fluid and Plasma Dynamics Conf., Palo Alto, AIAA-81-1259, 1981.
7. Fennema R.J. and M.H. Chaudhry : Explicit methods for 2-D transient free-surface flows, Journal of Hydraulic Engineering, Vol.116, No.8, pp.1013-1034, 1990.
8. Akiyama J., M. Ura, M. Yamaguchi and M. Shigeeda : Applicability of 2-D numerical model on MacCormack scheme to shallow water flow, Annual Journal of Hydraulic Engineering, JSCE, Vol.42, pp/679-684, 1998. (in Japanese)
9. Report of Experiments on the Asahi river: Public Works Research Center, pp.152, 1992. (in Japanese)

APPENDIX-NOTATION

The following symbols are used in this paper :

$\mathbf{A}$ = vector of flow variables ;

$\mathbf{B}, \mathbf{C}$ = vectors of fluxes in ξ and η direction ;

C_r = Courant number

$\mathbf{D}$, = vector of source terms ;

g = gravity acceleration ;

h = water depth ;

J = Jacobean of coordinate transform ($J = \xi_x \eta_y - \xi_y \eta_x$) ;

k = damping paramerer used in artificial viscosity term ;

ℓ_ξ, ℓ_η = space increment used in viscosity term ;

L_ξ, L_η = differencing operator in ξ, η direction ;

n = coefficient of Manning's roughness ;

Q = discharge

$\mathbf{R}, \mathbf{T}$ = vectors of diffusion terms ;

u, v = velocities in x, y direction ;

u', v' = velocities in ξ, η direction (contravariant velocities) ;

u_* = shear velocity ;
x, y = axes in Cartesian coordinates ;
z = bed level ;
α = parameter used in eddy viscosity term;
γ = paramerer used in artificial viscosity term ;
Δt = time increment
$\Delta\xi, \Delta\eta$ = space increment in ξ, η direction ;
ε = coefficient of eddy viscosity ;
κ = von Karman constant ;
ν = paramerer used in artificial viscosity term ; and
ξ, η = axes in curvilinear coordinates.

Superscripts

c = corrector stage ;
n = time increment ;
p = predictor stage ; and
ξ, η = variables in ξ, η direction.

Subscripts

i, j = grid indices ;
t = differentiation with respect to t ; and
ξ, η = differentiation with respect to ξ, η .

(Received August 10, 2000 ; revised December 22, 2000)